

A Radial Basis Function Galerkin Method for Anisotropic Nonlocal Diffusion[☆]

R. B. Lehoucq^{a,*}, S. T. Rowe^b

^a*Computational Mathematics, Sandia National Laboratories, Albuquerque, NM 87185-1320, USA*

^b*Department of Mathematics, Texas A&M University, College Station, TX 77843-3368, USA*

Abstract

We introduce a discretization for a nonlocal diffusion problem using a localized basis of radial basis functions. The stiffness matrix entries are assembled by a special quadrature routine unique to the localized basis. Combining the quadrature method with the localized basis produces a well-conditioned, sparse, symmetric positive definite stiffness matrix. We demonstrate that both the continuum and discrete problems are well-posed and present numerical results for the convergence behavior of the radial basis function method. We explore approximating the solution to anisotropic differential equations by solving anisotropic nonlocal integral equations using the radial basis function method.

Keywords: Nonlocal diffusion, radial basis functions, nonlocal vector calculus, Lagrange functions

1. Introduction

The purpose of this paper is to introduce a meshfree method for the solution of an anisotropic nonlocal diffusion equation. We apply a recently developed approximation and interpolation scheme to construct a discretization space. We introduce a quadrature method unique to the discretization that enables assembly of a sparse stiffness matrix. The entries in the stiffness matrix are computed by pointwise evaluations of a kernel and multiplication by quadrature weights. In contrast, evaluating entries in the stiffness matrix for a piecewise polynomial

[☆]The work of the authors was supported by the Laboratory Directed Research and Development (LDRD) program at Sandia National Laboratories. Sandia is a multi-program laboratory managed and operated by Sandia Corporation, a wholly subsidiary of Lockheed Martin Corporation, for the U.S. Department of Energy's National Nuclear Security Administration under contract DE-AC04-94AL85000

*Corresponding author

Email addresses: rblehou@sandia.gov (R. B. Lehoucq), srowe@math.tamu.edu (S. T. Rowe)

finite element discretization remains a challenging quadrature problem. Evaluating entries in the stiffness matrix for a problem in \mathbb{R}^n requires $2n$ -iterated integrals over partial element volumes. The paper [1] explored radial basis function methods for the discretization of the nonlocal diffusion equation by a localized basis and an associated quadrature routine. The approach presented in this paper reduces the computational difficulty of both the construction of the quadrature weights and the evaluation of the solution on a set of points. In particular, our approach maintains the same benefits of the radial basis function method in [1] while avoiding the solution of large, dense linear systems. Moreover, we extend the results of [1] by considering anisotropic nonlocal diffusion equations and demonstrating that both the continuum and discrete problems are well-posed.

Section 2 briefly discusses aspects of the nonlocal vector calculus we require to formulate the nonlocal diffusion problem. We also consider comparisons with the classical diffusion problem. Section 3 discusses radial basis functions that are used in the construction of the discretization space. Section 3.1 introduces the local Lagrange functions that are used to produce the approximation spaces for the discretization method. The quadrature method unique to the discretization is introduced in Section 4. Section 5 introduces the discretization method for the nonlocal diffusion problem and investigates theoretical properties of the method. Numerical experiments for the discretization of the nonlocal diffusion problem are discussed in Section 6. In addition to studying the discretization of nonlocal diffusion problems, Section 6.3 presents experiments that consider approximating the solution to an anisotropic differential equation by discretizing and solving an anisotropic nonlocal diffusion problem. For notation, we let bold lower case letters indicate vectors and unbolded lower case letters indicate scalars. Bold upper case letters are reserved for operators and matrices.

2. Nonlocal Vector Calculus

In this section, we present topics from the nonlocal vector calculus required to define the nonlocal diffusion equation. The nonlocal vector calculus developed in [7] provides nonlocal analogues of classical operators such as the gradient, divergence, and curl operators.

Let $\nu(\mathbf{x}, \mathbf{y}), \alpha(\mathbf{x}, \mathbf{y}) : \mathbb{R}^n \times \mathbb{R}^n \rightarrow \mathbb{R}^k$ where α is an anti-symmetric mapping, i.e., $\alpha(\mathbf{x}, \mathbf{y}) = -\alpha(\mathbf{y}, \mathbf{x})$. The nonlocal divergence operator \mathcal{D} acts on ν by

$$(\mathcal{D}\nu)(\mathbf{x}) := \int_{\mathbb{R}^n} (\nu(\mathbf{x}, \mathbf{y}) + \nu(\mathbf{y}, \mathbf{x})) \cdot \alpha(\mathbf{x}, \mathbf{y}) d\mathbf{y}.$$

The adjoint operator \mathcal{D}^* acts on $u(\mathbf{x}) : \mathbb{R}^n \rightarrow \mathbb{R}$ pointwise by

$$\mathcal{D}^*(u)(\mathbf{x}, \mathbf{y}) = -(u(\mathbf{y}) - u(\mathbf{x}))\alpha(\mathbf{x}, \mathbf{y}) \quad \text{for } \mathbf{x}, \mathbf{y} \in \mathbb{R}^n,$$

where $\mathcal{D}^*u : \mathbb{R}^n \times \mathbb{R}^n \rightarrow \mathbb{R}^k$.

For an open subset $\Omega \subset \mathbb{R}^n$, we define the interaction domain

$$\Omega_{\mathcal{I}} := \{\mathbf{y} \in \mathbb{R}^n \setminus \Omega : \alpha(\mathbf{x}, \mathbf{y}) \neq 0 \text{ for some } \mathbf{x} \in \Omega\}. \quad (1)$$

Given $f : \Omega \rightarrow \mathbb{R}$ and $g : \Omega_{\mathcal{I}} \rightarrow \mathbb{R}$, we are interested in solving the weak formulation of the steady-state nonlocal diffusion problem

$$\begin{cases} \mathcal{L}u = f & \text{on } \Omega, \\ u = g & \text{on } \Omega_{\mathcal{I}}, \end{cases} \quad (2)$$

where $\Theta(\mathbf{x}, \mathbf{y})$ is a second-order tensor satisfying $\Theta = \Theta^T$, and the nonlocal diffusion operator is given by

$$\mathcal{L}u(\mathbf{x}) = 2 \int_{\Omega \cup \Omega_{\mathcal{I}}} (u(\mathbf{y}) - u(\mathbf{x})) \alpha(\mathbf{x}, \mathbf{y}) \cdot (\Theta(\mathbf{x}, \mathbf{y}) \cdot \alpha(\mathbf{x}, \mathbf{y})) d\mathbf{y}, \quad \mathbf{x} \in \Omega. \quad (3)$$

In contrast to classical diffusion models that impose boundary conditions, the nonlocal model enforces conditions over a positive measure volume, or a volume constraint. This constraint guarantees that the weak formulation of (2) is well-posed provided conditions on the kernel. For integrable kernels, the paper [2] demonstrates that (2) is well-posed on the space $L^2_c(\Omega \cup \Omega_{\mathcal{I}}) = \{u \in L^2(\Omega \cup \Omega_{\mathcal{I}}) : u|_{\Omega_{\mathcal{I}}} = 0 \text{ a.e.}\}$. Let $u \in L^2(\Omega \cup \Omega_{\mathcal{I}})$ and let $\gamma_\epsilon := \alpha \cdot \Theta \cdot \alpha$ be a radial kernel with support radius, or horizon, ϵ . Under general conditions, as $\epsilon \rightarrow 0$, the solution u_ϵ of (2) converges to the solution of

$$\begin{cases} \nabla \cdot \mathbf{C} \nabla u = f & \text{on } \Omega \\ u = g & \text{on } \partial\Omega, \end{cases} \quad (4)$$

where \mathbf{C} is a diffusion tensor. The interested reader should also consult [2, §3 pp.674-678] for further exposition on nonlocal operators, comparisons between nonlocal diffusion and classical diffusion equations, and comparisons with the classical vector calculus and the nonlocal calculus. The recent paper [3] discusses the nonlocal analogue of (4) with a Neumann boundary condition and relationship with a smoothed particle hydrodynamic approximation.

We now demonstrate that the solution u of the nonlocal diffusion equation (2) is the minimizer of a variational problem, the weak formulation of (2). Let $\Omega \subset \mathbb{R}^n$ be an open region and let $\Omega_{\mathcal{I}}$ be the corresponding interaction domain as defined in (1). The energy functional is defined to be

$$\begin{aligned} E(u; f) := & \frac{1}{2} \int_{\Omega \cup \Omega_{\mathcal{I}}} \int_{\Omega \cup \Omega_{\mathcal{I}}} \mathcal{D}^*(u)(\mathbf{x}, \mathbf{y}) \cdot (\Theta(\mathbf{x}, \mathbf{y}) \cdot \mathcal{D}^*(u)(\mathbf{x}, \mathbf{y})) d\mathbf{x} d\mathbf{y} \\ & - \int_{\Omega} f(\mathbf{x}) u(\mathbf{x}) d\mathbf{x} \end{aligned}$$

where f is a given function defined on Ω . Let $g(\mathbf{x})$ be a function defined on $\Omega_{\mathcal{I}}$ and let $E_c(u; g)$ denote the constraint functional

$$E_c(u; g) := \int_{\Omega_{\mathcal{I}}} (u(\mathbf{x}) - g(\mathbf{x}))^2 d\mathbf{x}. \quad (5)$$

We consider the constrained minimization problem

$$\min E(u; f) \quad \text{subject to} \quad E_c(u; g) = 0.$$

The constraint functional may be interpreted as a nonlocal Dirichlet volume constraint analogous to Dirichlet boundary conditions for differential equations. By considering test functions v that satisfy $E_c(v; 0) = 0$, we arrive at the necessary conditions for the minimization problem

$$\int_{\Omega \cup \Omega_{\mathcal{I}}} \int_{\Omega \cup \Omega_{\mathcal{I}}} \mathcal{D}^*(u)(\mathbf{x}, \mathbf{y}) \cdot (\Theta(\mathbf{x}, \mathbf{y}) \cdot \mathcal{D}^*(v)(\mathbf{x}, \mathbf{y})) \, d\mathbf{y} \, d\mathbf{x} = \int_{\Omega} f(\mathbf{x})v(\mathbf{x}) \, d\mathbf{x}. \quad (6)$$

To relate (6) to (2), we require a nonlocal analogue of Green's first identity. Define the interaction operator $\mathcal{N}(\nu) : \mathbb{R}^n \rightarrow \mathbb{R}$ by

$$\mathcal{N}(\nu)(\mathbf{x}) := - \int_{\Omega \cup \Omega_{\mathcal{I}}} (\nu(\mathbf{x}, \mathbf{y}) + \nu(\mathbf{y}, \mathbf{x})) \cdot \alpha(\mathbf{x}, \mathbf{y}) \, d\mathbf{y} \quad \text{for } \mathbf{x} \in \Omega_{\mathcal{I}}.$$

The nonlocal Green's first identity is

$$\int_{\Omega} v \mathcal{D}(\Theta \cdot \mathcal{D}^*u) \, d\mathbf{x} - \int_{\Omega \cup \Omega_{\mathcal{I}}} \int_{\Omega \cup \Omega_{\mathcal{I}}} (\mathcal{D}^*v) \cdot (\Theta \cdot \mathcal{D}^*u) \, d\mathbf{y} \, d\mathbf{x} = \int_{\Omega_{\mathcal{I}}} v \mathcal{N}(\Theta \cdot \mathcal{D}^*u) \, d\mathbf{x}. \quad (7)$$

We apply (7) to (6) and note that $v = 0$ in $\Omega_{\mathcal{I}}$ to obtain

$$\int_{\Omega} v(\mathbf{x}) \mathcal{D}(\Theta \cdot \mathcal{D}^*u)(\mathbf{x}) \, d\mathbf{x} = \int_{\Omega} f(\mathbf{x})v(\mathbf{x}) \, d\mathbf{x}. \quad (8)$$

Because v is arbitrary, the minimizer u satisfies

$$\begin{aligned} -\mathcal{L}u &= \mathcal{D}\Theta \cdot \mathcal{D}^*u = f && \text{on } \Omega, \\ u &= g && \text{on } \Omega_{\mathcal{I}}. \end{aligned}$$

2.1. Discretization of the Variational Problem

Let $\Omega \subset \mathbb{R}^n$ be an open region and let $\Omega_{\mathcal{I}}$ be the interaction domain corresponding to Ω , as defined in (1). Let $u, v \in L^2(\Omega \cup \Omega_{\mathcal{I}})$, $f \in L^2(\Omega)$, and $g \in L^2(\Omega_{\mathcal{I}})$. We define the nonlocal bilinear form $a(\cdot, \cdot)$

$$a(u, v) := \frac{1}{2} \int_{\Omega \cup \Omega_{\mathcal{I}}} \int_{\Omega \cup \Omega_{\mathcal{I}}} \mathcal{D}^*(u)(\mathbf{x}, \mathbf{y}) \cdot (\Theta(\mathbf{x}, \mathbf{y}) \cdot \mathcal{D}^*(v)(\mathbf{x}, \mathbf{y})) \, d\mathbf{y} \, d\mathbf{x}. \quad (9)$$

The nonlocal bilinear form induces a semi-norm $\|u\| = \sqrt{a(u, u)}$ on $L^2(\Omega \cup \Omega_{\mathcal{I}})$, which is equivalent to the $L^2(\Omega \cup \Omega_{\mathcal{I}})$ norm for functions restricted to the constrained energy space

$$L_c^2(\Omega \cup \Omega_{\mathcal{I}}) := \{u \in L^2(\Omega \cup \Omega_{\mathcal{I}}) : \|u\| < \infty \text{ and } u|_{\Omega_{\mathcal{I}}} = 0 \text{ a.e.}\}.$$

We seek $u \in L_c^2(\Omega \cup \Omega_{\mathcal{I}})$ such that for all $v \in L_c^2(\Omega \cup \Omega_{\mathcal{I}})$,

$$a(u, v) = \int_{\Omega} f(\mathbf{x})v(\mathbf{x}) \, d\mathbf{x}. \quad (10)$$

The coercivity and boundedness of the bilinear form on $L_c^2(\Omega \cup \Omega_{\mathcal{I}})$ along with the boundedness of the linear form on the right hand-side of (10) implies that the anisotropic problem is well-posed by the Lax-Milgram theorem on $L_c^2(\Omega \cup \Omega_{\mathcal{I}})$ [2, Lemma 4.7]. The problem is discretized by a finite-dimensional subspace $V_h = \text{span}\{\phi_i\}_{i=1}^N \subset L_c^2(\Omega \cup \Omega_{\mathcal{I}})$. The resulting discrete problem seeks $u_h = \sum_{i=1}^N c_i \phi_i \in V_h$ such that for all $v_h \in V_h$,

$$a(u_h, v_h) = \int_{\Omega} f(\mathbf{x}) v_h(\mathbf{x}) d\mathbf{x}.$$

The resulting linear system $\mathbf{A}\mathbf{c} = \mathbf{b}$ has entries given by

$$\mathbf{A}_{i,j} = a(\phi_i, \phi_j) \quad \mathbf{b}_i = \int_{\Omega} f(\mathbf{x}) \phi_i(\mathbf{x}) d\mathbf{x}. \quad (11)$$

In Section 5, we present a discretization using a localized basis of radial basis functions that generates a well-conditioned, sparse stiffness matrix.

In Section 6.3, we present numerical experiments that study the approximation of the solution to a differential equation by solving a discretized nonlocal anisotropic problem.

3. Radial Basis Functions

We discuss relevant background information on radial basis functions and interpolation in this section. Radial basis functions (RBFs) are used to construct the approximation space for the Galerkin method we propose in Section 5. Let $\Omega \subset \mathbb{R}^n$ and $\Phi : \Omega \rightarrow \mathbb{R}$ be a continuous function. We say that Φ is *radial* if there exists $\varphi : \mathbb{R}^+ \rightarrow \mathbb{R}$ such that $\Phi(\mathbf{x}) = \varphi(\|\mathbf{x}\|)$ for all $\mathbf{x} \in \mathbb{R}^n$. Let $\{\mathbf{x}_i\}_{i=1}^N = X \subset \Omega$ be a collection of scattered points, referred to as centers. A set of *radial basis functions* $\{\Phi_i\}_{i=1}^N$ is constructed by setting $\Phi_i(\mathbf{x}) = \Phi(\mathbf{x} - \mathbf{x}_i) = \varphi(\|\mathbf{x} - \mathbf{x}_i\|)$. Given a continuous function $f : \Omega \rightarrow \mathbb{R}$, an interpolant $I_X f = \sum_{i=1}^N c_i \Phi_i(\mathbf{x})$ is constructed by enforcing

$$f(\mathbf{x}_i) = \sum_{j=1}^N c_j \varphi(\|\mathbf{x}_i - \mathbf{x}_j\|) \quad i = 1, \dots, N, \quad (12)$$

provided that the resulting linear system of equations has a unique solution. We say a function Φ is positive definite if for any set of scattered points $\{\mathbf{x}_j\}_{j=1}^N$, the quadratic form $\sum_{i=1}^N \sum_{j=1}^N \alpha_i \alpha_j \Phi(\mathbf{x}_i - \mathbf{x}_j)$ is positive. This condition implies that equation (12) admits a unique solution for any set of centers. Examples of positive definite functions include the Gaussians $\varphi(r) = \exp(-\alpha r^2)$, the compactly supported Wendland functions, and the inverse multiquadrics $\varphi(r) = (r^2 + c^2)^{-\beta}$ for $\beta, c > 0$. The interested reader should consult [11] or [4] for further details on radial basis functions and interpolation.

The basis we construct in Section 3.1 requires *conditionally* positive definite functions. Let $\Pi_L(\mathbb{R}^n) = \text{span}\{p_l\}_{l=1}^{n_L}$ denote the space of polynomials of degree

less than L on \mathbb{R}^n . We say that $\varphi(r)$ is conditionally positive definite of order L if for any set of centers $\{\mathbf{x}_i\}_{i=1}^N$ and any $\boldsymbol{\alpha} \neq 0 \in \mathbb{R}^N$ satisfying $\sum_{i=1}^N \alpha_i p(\mathbf{x}_i) = 0$ for $p \in \Pi_L(\mathbb{R}^n)$, the quadratic form $\sum_{i=1}^N \sum_{j=1}^N \alpha_i \alpha_j \varphi(\|\mathbf{x}_i - \mathbf{x}_j\|)$ is positive. For example, the surface spline

$$\varphi(r) = \begin{cases} r^{2m-n} & n \text{ is odd} \\ r^{2m-n} \log(r) & n \text{ is even} \end{cases} \quad (13)$$

is conditionally positive definite of order m on \mathbb{R}^n . Conditionally positive definite RBFs can construct unique interpolants for scattered data provided additional polynomial constraints. Given centers $\{\mathbf{x}_i\}_{i=1}^N$ and data $\{f(\mathbf{x}_i)\}_{i=1}^N$, the interpolant $I_X f = \sum_{j=1}^N c_j \varphi(\|\mathbf{x} - \mathbf{x}_j\|) + \sum_{l=1}^{n_L} d_l p_l(\mathbf{x})$ is constructed by enforcing

$$\begin{aligned} f(\mathbf{x}_i) &= \sum_{j=1}^N c_j \varphi(\|\mathbf{x}_i - \mathbf{x}_j\|) + \sum_{l=1}^{n_L} d_l p_l(\mathbf{x}_i) && \text{for } i = 1, \dots, N, \\ 0 &= \sum_{j=1}^N c_j p_l(\mathbf{x}_j) && \text{for } l = 1, \dots, n_L. \end{aligned} \quad (14)$$

Constructing the coefficients for $I_X f$ requires solving an $(N + n_L) \times (N + n_L)$ dense, symmetric linear system. In section 3.1, an alternative radial basis function method that does not require the solution of a system of size $N + n_L$ is discussed.

The geometry of the centers is important for estimating the approximation quality of the RBF interpolant and for estimating the condition number of the interpolation matrix. RBF interpolation offers the advantage of not requiring regular distributions of points; arbitrarily scattered centers produce invertible interpolation matrices for positive definite functions. Let $X \subset \Omega \subset \mathbb{R}^n$ be a set of scattered centers. We define the *mesh norm* (or fill distance) h to be the radius of the largest ball in Ω that does not contain any centers and we define the *separation radius* q to be the minimal pairwise distance between the centers. See Figure 1 for a visual example of the mesh norm. These quantities are mathematically defined by

$$h = \sup_{\mathbf{x} \in \Omega} \min_{\mathbf{x}_j \in X} \|\mathbf{x} - \mathbf{x}_j\|, \quad q = \min_{\mathbf{x}_i, \mathbf{x}_j \in X} \|\mathbf{x}_i - \mathbf{x}_j\|, \quad \rho = \frac{h}{q}, \quad (15)$$

where the *mesh ratio* ρ provides a means of judging how well distributed the points are. Informally, for ρ near one, the centers are almost uniformly distributed and large ρ indicates clustering of centers. We say that collections of centers $\{X_{h,q}\}$ are *quasi-uniformly* distributed if there exists positive constants C_1, C_2 such that

$$C_1 q \leq h \leq C_2 q. \quad (16)$$

Geometrically, this condition controls how the centers cluster as the density of points increases. We note that for the quasi-uniformly distributed collections

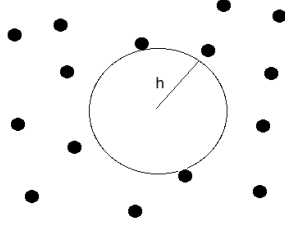


Figure 1: The mesh norm is the radius of the largest ball which does not contain any centers.

of centers $\{X_{h,q}\}$, we do not require that any of the point sets are nested in another.

The approximation error between f and $I_X f$ can be quantified in terms of the geometry of the scattered centers. Let $\varphi(r)$ denote the surface spline of order m on \mathbb{R}^n and let $W_2^k(\Omega)$ denote the Sobolev space of order k .

Theorem 1. [10, Theorem 4.2] Let $f \in W_2^\beta(\Omega)$ for $\frac{n}{2} < \beta \leq m$. Then, for any $0 \leq \mu < \beta$,

$$\|f - I_X f\|_{W_2^\mu(\Omega)} \leq Ch^{\beta-\mu} \|f\|_{W_2^\beta(\Omega)}. \quad (17)$$

3.1. Lagrange Functions and Local Lagrange Functions

We discuss a localized basis for interpolation and approximation using linear combinations of surface splines in this section. Let $X \subset \Omega$ be a set of N centers and let $\varphi(r)$ denote the surface spline of order m . For each $\mathbf{x}_i \in X$, there exists a unique interpolant χ_i that satisfies $\chi_i(\mathbf{x}_j) = \delta_{i,j}$. We refer to the basis $\{\chi_i(\mathbf{x})\}_{i=1}^N$ as the *Lagrange basis* and χ_i as the *Lagrange function* centered at \mathbf{x}_i . The interpolant to a continuous function f can be written as a linear combination of Lagrange functions and function samples by $I_X f = \sum_{i=1}^N f(\mathbf{x}_i)\chi_i(\mathbf{x})$. The χ_i functions are constructed by solving the $(N + n_L) \times (N + n_L)$ linear system (14) for each χ_i . This is a computational issue that has limited the exploration and use of Lagrange functions. Previous work used Lagrange functions for discretization of the nonlocal problem [1].

We discuss the construction of local Lagrange functions that are constructed more efficiently than the full Lagrange functions. The discretization we introduce in Section 5 uses local Lagrange functions for compact domains $\Omega \subset \mathbb{R}^n$. Let $X \subset \Omega$ be a set of scattered centers with mesh norm h and separation radius q and let $K > 0$ be a fixed constant. To construct the local Lagrange functions, additional centers outside of the domain Ω are included in a larger set of points $\Xi \supset X$. Let $\tilde{\Omega} = \{\mathbf{x} \in \mathbb{R}^n : d(\mathbf{x}, \Omega) \leq Kh|\log(h)|\}$. A set of centers Ξ can be constructed such that $\Xi \cap \Omega = X$ and Ξ has mesh norm h in $\tilde{\Omega}$. For each $\mathbf{x}_i \in X$, let $\Upsilon_i = \{\mathbf{y} \in \Xi : d(\mathbf{x}_i, \mathbf{y}) \leq Kh|\log(h)|\}$. The *local Lagrange function* centered at \mathbf{x}_i has the form

$$b_i(\mathbf{x}) = \sum_{\mathbf{y} \in \Upsilon_i} \alpha_{\eta,i} \varphi(\|\mathbf{x} - \mathbf{y}\|) + \sum_{l=1}^{n_L} \beta_{l,i} p_l(\mathbf{x}) \quad (18)$$

and the coefficients are constructed by solving

$$\begin{pmatrix} \mathbf{S}_i & \mathbf{P} \\ \mathbf{P}^T & 0 \end{pmatrix} \begin{pmatrix} \boldsymbol{\alpha}^i \\ \boldsymbol{\beta}^i \end{pmatrix} = \begin{pmatrix} \mathbf{e}_i \\ 0 \end{pmatrix} \quad (19)$$

where $\mathbf{S}_i(\mathbf{y}, \mathbf{z}) = \varphi(\|\mathbf{y} - \mathbf{z}\|)$ for $\mathbf{y}, \mathbf{z} \in \Upsilon_i$, $\mathbf{P}(\mathbf{y}, l) = p_l(\mathbf{y})$ and $\mathbf{e}_i(\mathbf{y}) = \delta(\mathbf{x}_i, \mathbf{y})$. The cardinality of Υ_i can be estimated by using the separation radius q and a volume estimate. Applying quasi-uniformity (16) and noting that every center is separated by at least q , we estimate

$$\#\Upsilon_i \leq \frac{\mu(B(\mathbf{x}_i, Kh|\log(h)|))}{\mu(B(\mathbf{x}_i, q))} \sim \frac{K^n h^n}{Cq^n} |\log(h)|^n \leq \tilde{C}\rho^n |\log(N)|^n.$$

For quasi-uniformly distributed sets of centers, $\frac{h}{q} := \rho$ is bounded above and below by fixed constants. Therefore, constructing a local Lagrange function requires solving linear systems of size $O(\log(N)^n)$ as opposed to $O(N)$ for the full Lagrange functions. The local Lagrange functions provide approximation rates analogous to known approximation rates for globally supported Lagrange functions.

Lemma 1. *Let $\frac{n}{2} < k \leq m$ and let $\Omega \cup \Omega_I \subset \mathbb{R}^n$. Let $f \in W_2^k(\Omega \cup \Omega_I)$ be a compactly supported function such that $f|_{\Omega_I} = 0$. Then, for sufficiently large K , the quasi-interpolant $\tilde{I}_X(f) = \sum_{i=1}^N f(\mathbf{x}_i)b_i$ satisfies*

$$\|f - \tilde{I}_X f\|_{L^2(\Omega)} \leq Ch^k \|f\|_{W_2^k(\Omega)}.$$

PROOF. We assume the set of centers $\Xi \subset \Omega \cup \Omega_I$ with $X := \Xi \cap \Omega$. Let χ_i be the Lagrange functions centered at \mathbf{x}_i and b_i denote the local Lagrange function centered at \mathbf{x}_i . Then,

$$\begin{aligned} \|u - \sum_{i=1}^N u(\mathbf{x}_i)b_i\|_{L^2(\Omega \cup \Omega_I)} &\leq \|u - \sum_{i=1}^N u(\mathbf{x}_i)\chi_i\|_{L^2(\Omega \cup \Omega_I)} \\ &\quad + \left\| \sum_{i=1}^N u(\mathbf{x}_i)(\chi_i - b_i) \right\|_{L^2(\Omega \cup \Omega_I)}. \end{aligned}$$

We note that $\sum_{i=1}^N u(\mathbf{x}_i)\chi_i$ is the Lagrange function interpolant to u using the set of centers in $\Xi \subset \Omega \cup \Omega_I$, and hence we may apply radial basis function error estimates (17) on $\Omega \cup \Omega_I$ to find

$$\|u - \sum_{i=1}^N u(\mathbf{x}_i)\chi_i\|_{L^2(\Omega \cup \Omega_I)} \leq Ch^k \|u\|_{W_2^k(\Omega \cup \Omega_I)}.$$

Next, we apply Theorem 4.10 [8] to bound $\|b_\xi - \chi_\xi\|_{L^2(\Omega \cup \Omega_I)}$. Noting that $N \leq Cq^{-d}$ for quasi-uniformly distributed sets and applying the Sobolev embedding theorem to bound $\|u\|_{L^\infty(\Omega \cup \Omega_I)} \leq C\|u\|_{W_2^k(\Omega \cup \Omega_I)}$, we compute

$$\begin{aligned} \left\| \sum_{i=1}^n u(\mathbf{x}_i)(b_i - \chi_i) \right\|_{L^2(\Omega \cup \Omega_I)} &\leq Cq^{-n} \|u\|_{\ell^2(N)} \sup_i \|b_i - \chi_i\|_{L^2(\Omega \cup \Omega_I)} \\ &\leq q^{-2n} \|u\|_{L^\infty(\Omega \cup \Omega_I)} h^{K\nu \setminus 2 - 4m + 2n - 2\tau - 1} \\ &\leq Ch^{K\nu \setminus 2 - 4m - 2\tau - 1} \|u\|_{W_2^k(\Omega \cup \Omega_I)}. \end{aligned}$$

Therefore, for sufficiently large K , the exponent on the h term is at least as large as k . Combining the two inequalities yields the result.

We sometimes refer to the Lagrange function at \mathbf{x}_i as the *full* or *global* Lagrange function to contrast it with the local Lagrange function at \mathbf{x}_i , which is constructed using only points near \mathbf{x}_i . Local Lagrange functions were first introduced on the sphere [5] where decay properties, quasi-interpolation convergence rates, and preconditioners were studied. The local Lagrange basis can be constructed in parallel by solving small (relative to the number of centers) linear systems. This should be contrasted with previous radial basis function methods that require solving large dense linear systems. Recent work by [8] has extended theoretical properties of the local Lagrange basis to compact domains in \mathbb{R}^n .

4. Local Lagrange Quadrature

We introduce a quadrature method for compactly supported functions in Ω that is essential for the implementation of the Galerkin method we introduce in Section 5. Let $f \in W_2^\beta(\Omega)$ be compactly supported in Ω and let $X \subset \Omega$ be a collection of N centers. Let $\chi_i(\mathbf{x})$ be a globally supported Lagrange function centered at $\mathbf{x}_i \in X$ and let b_i be a local Lagrange function centered at \mathbf{x}_i . We define the quadrature weight at \mathbf{x}_i to be $w_i = \int_\Omega \chi_i(\mathbf{x}) d\mathbf{x}$ and the *Lagrange function quadrature rule* to be $Q_X(f) = \sum_{i=1}^N f(\mathbf{x}_i)w_i$. Similarly, we define the *local* quadrature weight at \mathbf{x}_i to be $\hat{w}_i = \int_\Omega b_i(\mathbf{x}) d\mathbf{x}$ and the local quadrature method $\hat{Q}_X(f) = \sum_{i=1}^N f(\mathbf{x}_i)\hat{w}_i$. We demonstrate that the quadrature error decreases as the mesh norm decreases.

Lemma 2. *Let $f \in W_2^\beta(\Omega)$ be compactly supported for $\frac{n}{2} < \beta \leq m$. Then, for sufficiently large K ,*

$$\left| \int_\Omega f(\mathbf{x}) - \hat{Q}_X f \right| \leq Ch^\beta \|f\|_{W_2^\beta(\Omega)}.$$

PROOF. The result follows by the Cauchy-Schwarz inequality along with Lemma 1.

$$\begin{aligned} \left| \int_{\Omega} f(\mathbf{x}) d\mathbf{x} - \hat{Q}_X(f) \right| &= \left| \int_{\Omega} f(\mathbf{x}) d\mathbf{x} - \sum_{i=1}^N f(\mathbf{x}_i) \hat{w}_i \right| \\ &\leq \int_{\Omega} |f(\mathbf{x}) - \sum_{i=1}^N f(\mathbf{x}_i) b_i(\mathbf{x})| d\mathbf{x} \leq \sqrt{\mu(\Omega)} \|f - \hat{I}_X f\|_{L^2(\Omega)} \\ &\leq C \sqrt{\mu(\Omega)} h^\beta \|f\|_{W_2^\beta(\Omega)}. \end{aligned}$$

The Lagrange function quadrature rule was first proposed in [6] for manifolds without boundary. The proposed quadrature method enabled the use of arbitrarily scattered data samples for quadrature on spheres. Although the quadrature weights they proposed required solving a dense linear system, the local Lagrange basis provided a pre-conditioner for the quadrature weight system that resulted in a practical quadrature routine [5, Section 7]. The Lagrange function quadrature routine has been used for Galerkin methods for partial differential equations on spheres in [9]. In [1], a quadrature rule for compact domains was introduced by modifying the construction on manifolds. The quadrature method we introduced is a modification of the method of [1].

The Lagrange function quadrature weights can be constructed without computing the Lagrange functions. Let $\varphi(r)$ denote the surface spline of order m on \mathbb{R}^n from equation (13). For a set of centers $X \subset \Omega$, the Lagrange function quadrature weights are constructed by solving the linear system

$$\begin{pmatrix} \mathbf{T} & \mathbf{P} \\ \mathbf{P}^T & 0 \end{pmatrix} \begin{pmatrix} \mathbf{w} \\ \mathbf{d} \end{pmatrix} = \begin{pmatrix} \boldsymbol{\nu} \\ \boldsymbol{\eta} \end{pmatrix} \quad (20)$$

where $T_{i,j} = \varphi(\|\mathbf{x}_i - \mathbf{x}_j\|)$, $P_{i,l} = p_l(\mathbf{x}_i)$, $\boldsymbol{\nu}_i = \int_{\Omega} \varphi(\|\mathbf{x} - \mathbf{x}_i\|) d\mathbf{x}$, $\boldsymbol{\eta}_i = \int_{\Omega} p_l(\mathbf{x}) d\mathbf{x}$ and w_i is the quadrature weight at \mathbf{x}_i . This requires solving a dense, symmetric linear system of size $O(N)$ where N is the number of centers. The system (20) can be preconditioned by using the local Lagrange functions as described in [6]. We present an alternative method of producing quadrature weights by using the local Lagrange functions directly.

The local quadrature weights are constructed by computing the integrals of the translates $\varphi(\|\mathbf{x} - \mathbf{x}_i\|)$. Recall that by equation (18)

$$b_i(\mathbf{x}) = \sum_{\mathbf{y} \in \Upsilon_i} \alpha_{\mathbf{y}, \mathbf{x}_i} \varphi(\|\mathbf{x} - \mathbf{y}\|) + \sum_{l=1}^{n_L} \beta_{l,i} p_l(\mathbf{x})$$

and consequently,

$$\hat{w}_i = \sum_{\mathbf{y} \in \Upsilon_i} \alpha_{\mathbf{y}, \mathbf{x}_i} \int_{\Omega} \varphi(\|\mathbf{x} - \mathbf{y}\|) d\mathbf{x} + \sum_{l=1}^{n_L} \beta_{l,i} \int_{\Omega} p_l(\mathbf{x}) d\mathbf{x}. \quad (21)$$

The construction of the local quadrature weights does not require the solution of a large linear system, in contrast to the quadrature method introduced in

[1]. However, (21) does require that the local Lagrange function coefficients are computed before the weights can be constructed. After constructing the local Lagrange functions, the weights can be assembled in parallel.

5. Galerkin Radial Basis Function Method

We propose a local Lagrange Galerkin method for the discretization of (11). The stiffness matrix entries are evaluated by the local Lagrange quadrature method introduced in Section 4. Applying the local Lagrange quadrature results in a sparse stiffness matrix, where the sparsity pattern is governed by the horizon ϵ of the kernel. The quadrature formula for the entries requires a pointwise evaluation of the kernel and multiplication by the quadrature weights. In contrast, a piecewise polynomial finite element method for a $\Omega \subset \mathbb{R}^n$ requires the evaluation of $2n$ -iterated integrals over partial element volumes. The resulting quadrature problem is a nontrivial computational challenge. Issues relating to integration over partial element volumes do not arise in the Galerkin radial basis function method.

Previous work has explored a Galerkin radial basis function method using full Lagrange functions and an associated Lagrange function quadrature rule [1]. The difference between the method of [1] and our present work is in the discretization space and the assembly of the quadrature weights. Assembling the quadrature weights using the full Lagrange functions requires the solution of a dense linear system of size $O(N)$ where N is the number of basis functions in the discretization. Furthermore, evaluating the solution required solving another dense linear system of size $O(N)$. In contrast, the local Lagrange function method requires solving small linear systems of size $O(\log(N)^n)$ for centers in \mathbb{R}^n .

5.1. Local Lagrange Discretization

Let Ω be an open region and $\Omega_{\mathcal{I}}$ be the corresponding interaction domain. Let $X \subset \Omega \cup \Omega_{\mathcal{I}}$ be a set of quasi-uniformly scattered centers with mesh norm h . As described in Section 3.1, an extended set of centers $X' \supset X$ can be constructed such that $X' \cap (\Omega \cup \Omega_{\mathcal{I}}) = X$ and $h(X') = h$, and $\sup_{\mathbf{x}' \in X', \mathbf{x}_i \in X} \|\mathbf{x}' - \mathbf{x}_i\| \leq Kh|\log(h)|$ for fixed integer $K > 0$. For each $\mathbf{x}_i \in X$, we construct b_i , the local Lagrange function centered at \mathbf{x}_i . Let $V_h = \text{span}\{b_i : \mathbf{x}_i \in \Omega\}$. The space $V_h \not\subset L_c^2(\Omega \cup \Omega_{\mathcal{I}})$ because elements in V_h are necessarily nonzero in $\Omega_{\mathcal{I}}$. To guarantee that the method is conforming, we replace b_i with $\tilde{b}_i = b_i \mathbb{1}_{\Omega}$, where $\mathbb{1}_{\Omega}$ is an indicator function for Ω . Since the space \tilde{V}_h is conforming with respect to the bilinear form a from Equation (9), there exists $u_h \in \tilde{V}_h$ such that $a(u_h, v_h) = \int_{\Omega} f(\mathbf{x})v_h(\mathbf{x}) d\mathbf{x}$ for all $v_h \in \tilde{V}_h$. We demonstrate an error estimate which matches the interpolation error estimate we expect from using the local Lagrange functions for interpolation of the solution u .

Proposition 1. *Let $u \in W_2^k(\Omega)$ for $k > \frac{n}{2}$ be the solution to the nonlocal problem (10). Let u_h be the discrete solution from the restricted local Lagrange method. Then, for sufficiently small h and for sufficiently large K ,*

$$\|u - u_h\|_{L^2(\Omega \cup \Omega_{\mathcal{I}})} \leq Ch^k \|u\|_{W_2^k(\Omega \cup \Omega_{\mathcal{I}})} \quad (22)$$

PROOF. By the Lax-Milgram theorem, the discrete solution u_h satisfies $\|u - u_h\|_{L^2(\Omega \cup \Omega_{\mathcal{I}})} \leq C \inf_{v_h \in U_h} \|u - v_h\|_{L^2(\Omega \cup \Omega_{\mathcal{I}})}$. By setting $v_h = \sum_{i=1}^N u(\mathbf{x}_i) \tilde{b}_i$, we have

$$\begin{aligned} \|u - u_h\|_{L^2(\Omega \cup \Omega_{\mathcal{I}})} &\leq C \|u - \sum_{i=1}^N u(\mathbf{x}_i) \tilde{b}_i\|_{L^2(\Omega \cup \Omega_{\mathcal{I}})} = C \|u - \sum_{i=1}^N u(\mathbf{x}_i) b_i\|_{L^2(\Omega)} \\ &\leq C \|u - \sum_{i=1}^N u(\mathbf{x}_i) b_i\|_{L^2(\Omega \cup \Omega_{\mathcal{I}})}. \end{aligned}$$

Since $u \in L_c^2(\Omega \cup \Omega_{\mathcal{I}})$ it is compactly supported and hence we may apply Lemma 1 to compute

$$\|u - u_h\|_{L^2(\Omega \cup \Omega_{\mathcal{I}})} \leq Ch^k \|u\|_{W_2^k(\Omega \cup \Omega_{\mathcal{I}})}.$$

If we let $\mathbf{A}_{i,j} := a(\tilde{b}_i, \tilde{b}_j)$ denote the stiffness matrix generated by applying the bilinear form to the local Lagrange functions, we demonstrate that the condition number is bounded independent of the mesh norm h or the separation radius q .

Lemma 3. *The condition number of the discrete stiffness matrix \mathbf{A} is bounded above by a constant independent of h and q .*

PROOF. Let \mathbf{A} denote the $N \times N$ symmetric stiffness matrix and let $\mathbf{c} \in \mathbb{R}^N$. Then,

$$\langle \mathbf{A}\mathbf{c}, \mathbf{c} \rangle = \sum_{i=1}^N \left(\sum_{j=1}^N A_{i,j} c_j \right) c_i = a \left(\sum_{i=1}^N c_i \tilde{b}_i, \sum_{j=1}^N c_j \tilde{b}_j \right).$$

By the coercivity of the bilinear form and since $\sum_{i=1}^N c_i \tilde{b}_i \in L_c^2(\Omega \cup \Omega_{\mathcal{I}})$, there exists λ_1, λ_2 such that

$$\lambda_1 \left\| \sum_{i=1}^N c_i \tilde{b}_i \right\|_{L^2(\Omega \cup \Omega_{\mathcal{I}})} \leq a \left(\sum_{i=1}^N c_i \tilde{b}_i, \sum_{j=1}^N c_j \tilde{b}_j \right) \leq \lambda_2 \left\| \sum_{i=1}^N c_i \tilde{b}_i \right\|_{L^2(\Omega \cup \Omega_{\mathcal{I}})}.$$

It follows that since $\tilde{b}_i = 0$ on $\Omega_{\mathcal{I}}$ and $\tilde{b}_i|_{\Omega} = b_i$,

$$\lambda_1 \left\| \sum_{i=1}^N c_i \tilde{b}_i \right\|_{L^2(\Omega \cup \Omega_{\mathcal{I}})} = \lambda_1 \left\| \sum_{i=1}^N c_i b_i \right\|_{L^2(\Omega)}.$$

By [8, Proposition 5.3] and [8, Theorem 4.12], there exists C_Ω and $C_{\Omega \cup \Omega_{\mathcal{I}}}$ independent of h and q such that

$$C_\Omega q^n \|\mathbf{c}\|_{\ell^2(N)} \leq \left\| \sum_{i=1}^N c_i \mathbf{b}_i \right\|_{L^2(\Omega)} \quad \left\| \sum_{i=1}^N c_i \mathbf{b}_i \right\|_{L^2(\Omega \cup \Omega_{\mathcal{I}})} \leq C_{\Omega \cup \Omega_{\mathcal{I}}} q^n \|\mathbf{c}\|_{\ell^2(N)}.$$

Then, we bound

$$\text{cond}(\mathbf{A}) \leq \frac{\lambda_{\max}(\mathbf{A})}{\lambda_{\min}(\mathbf{A})} \leq \frac{C_{\Omega \cup \Omega_{\mathcal{I}}} \lambda_2}{C_\Omega \lambda_1}.$$

5.2. Assembling the stiffness matrix by quadrature

We discuss a practical method to assemble the elements of the discrete stiffness matrix. We form the discrete stiffness matrix by evaluating $a(\tilde{\mathbf{b}}_i, \tilde{\mathbf{b}}_j)$ for each $\mathbf{x}_i, \mathbf{x}_j \in X \cap \Omega$. The integrals are computed by applying the local Lagrange quadrature rule introduced in Section 4. The stiffness matrix $\mathbf{A}_{i,j} = a(\tilde{\mathbf{b}}_i, \tilde{\mathbf{b}}_j)$ is approximated by

$$\mathbf{A}_{i,j} \approx 2\delta_{i,j} \hat{w}_i \int_{\Omega \cup \Omega_{\mathcal{I}}} \gamma(\mathbf{x}, \mathbf{x}_i) d\mathbf{x} - 2\hat{w}_i \hat{w}_j \gamma(\mathbf{x}_i, \mathbf{x}_j). \quad (23)$$

The integral involving $\gamma(\mathbf{x}, \mathbf{x}_i)$ may be computed analytically for some kernels or by quadrature. We compute the values \mathbf{b}_i from (11) by applying the Lagrange function quadrature rule

$$\mathbf{b}_i \approx f(\mathbf{x}_i) \hat{w}_i \mathbb{1}_\Omega(\mathbf{x}_i). \quad (24)$$

Applying the quadrature rule results in a sparse stiffness matrix. It follows that $\mathbf{A}_{i,j} = 0$ for centers such that $\|\mathbf{x}_i - \mathbf{x}_j\| \geq \epsilon$ due to the compact support of γ . The horizon ϵ of γ and the mesh norm h determines the number of nonzero entries per row. If the quadrature rule is not used, the resulting stiffness matrix is dense due to the nonzero values the local Lagrange functions assume throughout Ω . We demonstrate that the density of nonzero elements in the stiffness matrix is bounded independent of h, q .

Lemma 4. *Let $\{X\}_{h,q}$ be a collection of quasi-uniformly distributed centers in \mathbb{R}^n . Then, the ratio of the number of nonzero entries per row to the total number of columns is bounded independent of h, q .*

PROOF. Fix $X := X_{h,q}$ and fix $\mathbf{x}_i \in X$. Recall that $\|\mathbf{x}_i - \mathbf{x}_j\| \geq \epsilon$, $\mathbf{A}_{i,j} = 0$ by (23). Let $N_i = \{\mathbf{x}_j : \|\mathbf{x}_j - \mathbf{x}_i\| \leq \epsilon\}$. Let C_n denote the constant so that a ball of radius r has volume $C_n r^n$. The number of nonzero entries on row i is the same as the cardinality of N_i , which we compute by estimating the number of centers in N_i . We bound the cardinality of N_i , denoted $\#N_i$, above by noting that every center is separated by at least q , so

$$C_n (\#N_i) q^n = \cup_{\mathbf{x}_j \in N_i} \mu(B(\mathbf{x}_i, q)) \geq \mu(B_\epsilon(\mathbf{x}_i)) = C_n \epsilon^n$$

which implies $\#N_i \leq \epsilon^n q^{-n}$. The density per row is computed by $\frac{\#N_i}{N} \leq \frac{\epsilon^n q^{-n}}{N}$. We bound N by noting that we may cover Ω with balls of radius h by

$\Omega \subset \cup_{\mathbf{x}_j \in X} B(\mathbf{x}_j, h)$. Consequently, $\mu(\Omega) \leq NC_n h^n$, which implies $N \geq \frac{\mu(\Omega)}{C_n h^n}$. Therefore,

$$\frac{N_i}{N} \leq \frac{\epsilon^n q^{-n}}{\mu(\Omega) C_n^{-n} h^{-n}} = \frac{C_n \epsilon^n h^n}{\mu(\Omega) q^n}.$$

The result follows by recalling that (16) bounds the mesh ratio $\frac{h}{q}$.

Let \tilde{u}_h denote the solution to the discretized linear system assembled by quadrature from (23) and (24). Let u_h denote the solution to the the problem $a(u_h, v_h) = \int_{\Omega} f(\mathbf{x}) v_h(\mathbf{x}) d\mathbf{x}$ as described in Section 5.1. We desire an estimate that predicts the convergence rate of \tilde{u}_h to u in terms of h , as in Proposition 1. However, this requires a thorough analysis of the affect of quadrature on the solution to the resulting linear system of equations. By applying the triangle inequality and Proposition 1, we may estimate

$$\|u - \tilde{u}_h\|_{L^2} \leq \|u - u_h\| + \|u_h - \tilde{u}_h\|_{L^2} \leq Ch^k \|u\|_{W_2^k} + \|u_h - \tilde{u}_h\|_{L^2}.$$

Both u_h and \tilde{u}_h are linear combinations of local Lagrange functions with coefficients $\{\alpha_i\}_{i=1}^N$ and $\{\tilde{\alpha}_i\}_{i=1}^N$ respectively. In the numerical experiments we present in Section 6, we only produce the coefficients $\{\tilde{\alpha}_i\}_{i=1}^N$ since we apply quadrature to assemble the linear system of equations. The error between u_h and \tilde{u}_h may be quantified by

$$\|u_h - \tilde{u}_h\|_{L^2} = \left\| \sum_{i=1}^N (\alpha_i - \tilde{\alpha}_i) b_i \right\|_{L^2} \leq C q^n \|\alpha_i - \tilde{\alpha}_i\|_{\ell^2(N)}.$$

We do not currently have an estimate to bound $\|\alpha_i - \tilde{\alpha}_i\|_{\ell^2(N)}$. Despite the lack of theoretical justification, we demonstrate in Section 6 that the discrete solution produced by solving the linear system assembled by using quadrature follows an estimate of the form in Proposition 1. These results suggest $\|u - \tilde{u}_h\|_{L^2} \sim \|u - u_h\|_{L^2} \leq Ch^k \|u\|_{W_2^k}$.

6. Numerical Results

We present numerical results for experiments using the discretization described in Section 5. We discuss local Lagrange function construction, L^2 error computations, and condition number computations. We compare the theoretical prediction for L^2 convergence and condition numbers with observed results from numerical experiments. We consider solving two dimensional problems of the form (10) with a radial kernel Φ and two different anisotropy functions κ ; see Section 6.1 and Section 6.2. For all tests we consider zero Dirichlet volume constraints. The tests are computed on the set $\Omega \cup \Omega_{\mathcal{T}}$ where $\Omega = (0, 1) \times (0, 1)$ and $\Omega_{\mathcal{T}} = [-\frac{1}{4}, \frac{5}{4}] \times [-\frac{1}{4}, \frac{5}{4}] \setminus \Omega$. All computations are done in MATLAB and the condition numbers of the sparse stiffness matrices are approximated by the cond function. The sparse linear system is solved with either MATLAB's backslash operator or by conjugate gradient with a specified tolerance of 10^{-9} .

The number of iterations required for convergence for conjugate gradient did not vary as h decreased.

The local Lagrange functions are constructed with linear combinations of the surface spline $\varphi(r) = r^2 \log(r)$. Each local Lagrange function is constructed using approximately $11 \log(N)^2$ nearest neighbor centers, where N is the total number of centers in $\Omega \cup \Omega_{\mathcal{T}}$. The stiffness matrix for the nonlocal problem only requires Lagrange functions centered in Ω , although thin plate splines centered in $\Omega_{\mathcal{T}}$ are required for the construction of the local Lagrange functions as described in Section 3.1.

A kernel $\gamma(\mathbf{x}, \mathbf{y}) = (\kappa(\mathbf{x}) + \kappa(\mathbf{y}))\Phi(\|\mathbf{x} - \mathbf{y}\|)$ is chosen with fixed horizon ϵ and a solution $u \in L^2_c(\Omega \cup \Omega_{\mathcal{T}})$ is chosen for each numerical experiment. The source function f is manufactured by computing $\mathcal{L}u(\mathbf{x}_i) = f(\mathbf{x}_i)$ for each center \mathbf{x}_i . The values of $f(\mathbf{x}_i)$ are computed by using tensor products of Gauss-Legendre nodes to approximate the integral in Equation (3).

We study L^2 convergence of the discrete solution by constructing sets of uniformly spaced centers and sets of scattered centers with various mesh norms. Uniformly spaced collections of centers X_h are constructed using grid spacing $h = .04, .02, .014, .008$, and $.006$. Collections of scattered centers \tilde{X}_h are constructed by modifying centers in X_h by a random perturbation of magnitude at most $\frac{2h}{15}$. Local Lagrange functions for each collection of centers are constructed to build the discretization space. The convergence of the discrete solution u_h to the solution u is measured by plotting the L^2 norm of the error $\|u_h - u\|_{L^2(\Omega \cup \Omega_{\mathcal{T}})}$ against the mesh norm h . We expect for $u \in W_2^k(\Omega \cup \Omega_{\mathcal{T}})$ that $\|u - u_h\|_{L^2(\Omega)} \leq Ch^k \|u\|_{W_2^k(\Omega)}$ by Proposition 1.

6.1. Linear Anisotropy Experiment

We choose solution a u and a kernel γ with anisotropy function κ and radial function Φ given by

$$\begin{cases} u(\mathbf{x}) = \sin(2\pi x_1) \sin(2\pi x_2) \mathbb{1}_{\Omega}(\mathbf{x}) \\ \kappa(\mathbf{x}) = 1 + x_1 + x_2 \\ \Phi(\|\mathbf{x} - \mathbf{y}\|) = \exp\left(-\frac{1}{1 - \frac{\epsilon}{2}\|\mathbf{x} - \mathbf{y}\|^2}\right) \end{cases} \quad (25)$$

and we discretize (10) with local Lagrange functions.

Figure 2 displays the observed L^2 convergence rates with respect to the mesh norm h for the uniformly spaced and scattered centers experiments. The log of the computed L^2 error versus the log of the mesh norm is presented along with a best fit line to estimate the convergence order of the observed data. Table 1 displays the condition numbers of the discrete stiffness matrices. The observed condition numbers of the stiffness matrices do not increase as the mesh norm decreases, which matches the result of Lemma 3.

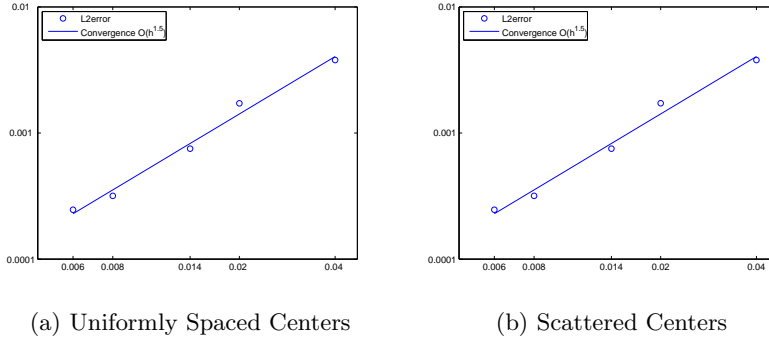


Figure 2: The log of h versus the log of the L^2 error for the linear anisotropic experiment with functions given by (25) is displayed.

6.2. Exponential Anisotropy Experiment

We choose solution u and a kernel γ with anisotropy function κ and radial function Φ given by

$$\begin{cases} u(\mathbf{x}) = \left(x_1(x_1 - 1)\right)^{\frac{1}{3}} \left(x_2(x_2 - 1)\right)^{\frac{1}{3}} \mathbb{1}_\Omega(\mathbf{x}) \\ \kappa_2(\mathbf{x}) = \exp(x_1 + x_2) \\ \Phi(\|\mathbf{x} - \mathbf{y}\|) = \exp\left(-\frac{1}{1 - \frac{1}{\epsilon^2}\|\mathbf{x} - \mathbf{y}\|^2}\right) \end{cases} \quad (26)$$

and we discretize (10) with local Lagrange functions.

Figure 3 displays the L^2 convergence plots for the experiments involving u_2 and κ_2 . The L^2 error rate matches the expected convergence rate predicted by Proposition 1. The expected h^2 order convergence is observed in both the uniformly spaced centers and the scattered centers experiments. Table 1 displays the condition numbers for the discrete stiffness matrices of various values for h . The condition numbers of the discrete stiffness matrices do not increase as the mesh norm decreases, which matches the prediction in Lemma 3.

6.3. Vanishing Nonlocality

We present numerical results for experiments that investigate the effects of shrinking the horizon ϵ . As discussed following (4), the solution of the nonlocal problem converges to the solution of (4) as ϵ decreases. We consider anisotropic kernels of the form

$$\gamma_\epsilon(\mathbf{x}, \mathbf{y}) = \frac{1}{\epsilon^3} (\kappa(\mathbf{x}) + \kappa(\mathbf{y})) \Phi\left(\frac{1}{\epsilon}\|\mathbf{x} - \mathbf{y}\|\right), \quad (27)$$

where $\Phi(\frac{1}{\epsilon}\|\mathbf{x}\|)$ is a compactly supported radial function with support radius ϵ . We investigate approximating the solution to an anisotropic differential equation by solving an anisotropic nonlocal problem with sufficiently small horizon ϵ .

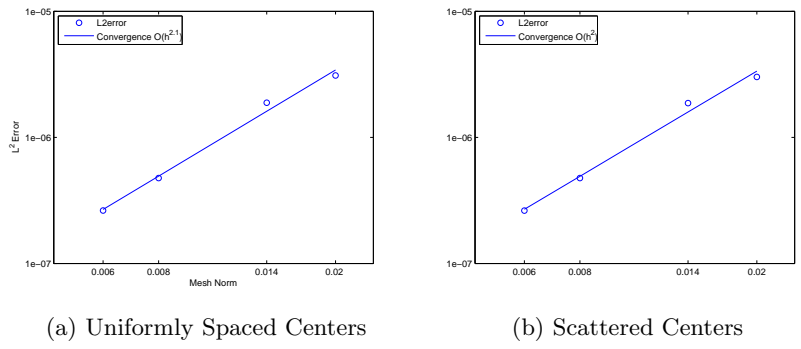


Figure 3: The log of h versus the log of the L^2 error for the exponential anisotropy experiment with functions given by (26) is displayed.

Table 1: The mesh norm h , number of rows n of the stiffness matrix, and the estimated condition number for the stiffness matrix with the linear anisotropy (25) and the exponential anisotropy (26). The condition numbers of the stiffness matrices does not increase as h decreases.

h	n	Approximate Condition Number	
		Linear	Exponential
2.83e-2	625	58	89
1.41e-2	2500	59	90
9.9e-3	5041	59	90
5.7e-3	15625	60	92
4.2e-3	27889	60	92

Numerical experiments demonstrate that the discrete solution to the anisotropic nonlocal problem converges to the solution of the anisotropic differential equation.

A Taylor series expansion argument can be used to find the differential operator D that the nonlocal operator approximates in the small horizon limit. We assume that $\kappa, u : \mathbb{R} \rightarrow \mathbb{R}$ are smooth functions. Then, for fixed $x \in \Omega$, we apply a Taylor series expansion in a ball $B_\epsilon(x)$ to obtain for some $\zeta, \eta \in B_\epsilon(x)$

$$u(y) - u(x) = u'(x)(y - x) + \frac{1}{2}u''(x)(y - x)^2 + \frac{1}{6}u''(\zeta)(y - x)^3$$

$$\kappa(x) + \kappa(y) = 2\kappa(x) + \kappa'(x)(y - x) + \kappa''(x)(y - x)^2 + \frac{1}{6}\kappa''(\eta)(y - x)^3.$$

If we denote by \mathcal{L}_ϵ the nonlocal operator with kernel γ_ϵ , then for smooth u , it follows that

$$\begin{aligned} \mathcal{L}_\epsilon u(x) &= \frac{1}{\epsilon^3} \left(2u'(x)\kappa(x) \int_{-\epsilon}^\epsilon z\Phi\left(\frac{1}{\epsilon}|z|\right) dz + u'(x)\kappa'(x) \int_{-\epsilon}^\epsilon z\Phi\left(\frac{1}{\epsilon}|z|\right) dz \right) \\ &\quad + \frac{1}{\epsilon^3} \left(2u''(x)\kappa(x) \int_{-\epsilon}^\epsilon z^2\Phi\left(\frac{1}{\epsilon}|z|\right) dz + u''(x)\kappa'(x) \int_{-\epsilon}^\epsilon z^3\Phi\left(\frac{1}{\epsilon}|z|\right) dz + \dots \right) \end{aligned}$$

where we have truncated the expression to exclude any of the $(y - x)^3$ terms. The $z\Phi(\frac{1}{\epsilon}|z|)$ integrals vanish since $z\Phi(\frac{1}{\epsilon}|z|)$ is an odd function. We exclude the z^3 integrals since

$$\frac{1}{\epsilon^3} \int_{-\epsilon}^\epsilon z^3\Phi\left(\frac{1}{\epsilon}|z|\right) dz \leq \frac{1}{2}\epsilon\|\Phi\|_{L^\infty(\Omega)},$$

which is $O(\epsilon)$. Eliminating these terms, we compute

$$\begin{aligned} \mathcal{L}_\epsilon u(x) &\approx 2(u'(x)\kappa'(x) + u''(x)\kappa(x)) \int_{-\epsilon}^\epsilon z^2\Phi\left(\frac{|z|}{\epsilon}\right) dz \\ &= 2(u'(x)\kappa'(x) + u''(x)\kappa(x)) \int_{-1}^1 \tau^2\Phi(|\tau|) d\tau. \end{aligned}$$

Therefore, as ϵ decreases to zero,

$$\begin{aligned} \mathcal{L}_\epsilon u(x) &\rightarrow \rho(u'(x)\kappa'(x) + u''(x)\kappa(x)) \\ \rho &:= 2 \int_{-1}^1 \tau^2\Phi(|\tau|) d\tau \end{aligned}$$

We numerically experiment with a Lagrange function discretization to solve the problem $\mathcal{L}_\epsilon u_\epsilon = f$ for anisotropic nonlocal operators. Let u denote the solution to $Du = f$ and let h be a given mesh norm. We solve $\mathcal{L}_\epsilon u_\epsilon = f$ by discretizing the problem with Lagrange functions to construct an approximate solution $u_{\epsilon,h}$. We numerically demonstrate that as $\epsilon \rightarrow 0$, $\|u - u_{\epsilon,h}\|_{L^2(\Omega \cup \Omega_T)} \sim O(\epsilon^2)$.

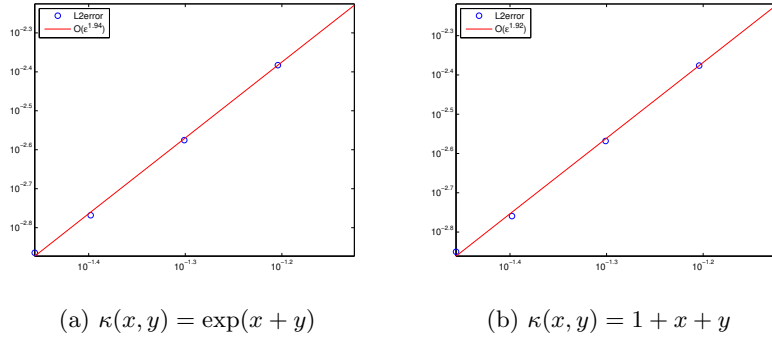


Figure 4: The log of ϵ vs. the log of the L^2 error of the discrete solution $u_{\epsilon,h}$ is plotted. As ϵ goes to zero, we observe ϵ^2 convergence.

We let $\Phi(\frac{1}{\epsilon}\|x\|) = (1 - \frac{1}{\epsilon^2}\|x\|^2)\mathbb{1}_{\|x\|<\epsilon}(x)$ and we consider two separate anisotropy functions $\kappa(x, y)$. We first consider a case of a linear anisotropic function of the form $\kappa_1(x, y) = 1 + x + y$ and $\kappa_2(x, y) = \exp(x + y)$. We set γ_ϵ as in (27) with the two choices for κ . The mesh norm $h = .000075$ is fixed for the experiments and we consider a range of ϵ values from .075, .0625, .05, .04, and .035. We discretize the problem $\mathcal{L}_\epsilon u_\epsilon = f$ with Lagrange functions and a discrete solution $u_{\epsilon,h}$ is computed as described in Section 5.

We choose

$$u(x) = (1 - \cos(2\pi x))\mathbb{1}_{[0,1]}(x) \tag{28}$$

and we analytically compute $Du = f$, where D is the differential operator that \mathcal{L}_ϵ converges to. We compute,

$$f(x) = \begin{cases} -2\pi(\sin(2\pi x) + 2\pi(1+x)\cos(2\pi x)) & \text{for } \kappa_1 \\ -\exp(x)(2\pi\sin(2\pi x) + 4\pi^2\cos(2\pi x)) & \text{for } \kappa_2 \end{cases}$$

In contrast to the experiments in Section 6.1 and Section 6.2, the source function f is fixed, h is fixed, and ϵ changes. The function f is chosen to be the solution to the problem $Du = f$, where u is the fixed function (28). As can be seen in Figure 4, for both κ_1 and κ_2 , the L^2 error $\|u - u_{\epsilon,h}\|_{L^2[0,1]}$ converges at about $O(\epsilon^2)$. The numerical results suggest it is possible to approximate the solution to an anisotropic differential equation by discretizing and solving an anisotropic nonlocal volume constrained equation.

[1] S. D. BOND, R. B. LEHOUCQ, AND S. T. ROWE, *A Galerkin radial basis function method for nonlocal diffusion*, Tech. Report SAND 2013-10673P, 2014. To Appear in the Proceedings of the Seventh International Workshop on Meshfree Methods for Partial Differential Equations; see the web page of R.B. Lehoucq for a copy.

- [2] Q. DU, M. GUNZBURGER, R. B. LEHOUCQ, AND K. ZHOU, *Analysis and approximation of nonlocal diffusion problems with volume constraints*, SIAM Review, 54 (2012), pp. 667–696.
- [3] Q. DU, R. LEHOUCQ, AND A. TARTAKOVSKY, *Integral approximations to classical diffusion and smoothed particle hydrodynamics*, Computer Methods in Applied Mechanics and Engineering, 286 (2015), pp. 216–229.
- [4] G. E. FASSHAUER, *Meshfree Approximation Methods with MATLAB*, World Scientific, 2007.
- [5] E. J. FUSELIER, T. HANGELBROEK, F. J. NARCOWICH, J. D. WARD, AND G. B. WRIGHT, *Localized bases for kernel spaces on the unit sphere*, SIAM J. Numer. Anal., 51 (2013).
- [6] ———, *Kernel based quadrature on spheres and other homogeneous spaces*, Numerische Mathematik, 127 (2014), pp. 57–92.
- [7] M. GUNZBURGER AND R. B. LEHOUCQ, *A nonlocal vector calculus with application to nonlocal boundary value problems*, SIAM Multiscale Modeling & Simulation, 8 (2010), pp. 1581–1598.
- [8] T. HANGELBROEK, F. J. NARCOWICH, C. RIEGER, AND J. D. WARD, *An inverse theorem on bounded domains for meshless methods using localized bases*, ArXiv e-prints, (2014).
- [9] F. J. NARCOWICH, S. T. ROWE, AND J. D. WARD, *A Novel Galerkin Method for Solving PDEs on the Sphere Using Highly Localized Kernel Bases*, ArXiv e-prints, (2014).
- [10] F. J. NARCOWICH, J. D. WARD, AND H. WENDLAND, *Sobolev error estimates and a Bernstein inequality for scattered data interpolation via radial basis functions*, Constructive Approximation, 24 (2006), pp. 175–186.
- [11] H. WENDLAND, *Scattered Data Approximation*, Cambridge University Press, 2005.